A R C H I V E S O F M E T A L L U R G Y A N D M A T E R I A L S
Volume 58 2013 Issue 4
DOI: 10.2478/amm-2013-0147

B. PAWŁOWSKI*, P. BAŁA*, T. TOKARSKI*, J. KRAWCZYK*

PREMATURE CRACKING OF DIES FOR ALUMINIUM ALLOY DIE-CASTING

PRZEDWCZESNE PĘKANIE MATRYC DO CIŚNIENIOWEGO ODLEWANIA STOPÓW ALUMINIUM

Two identical dies for aluminium alloy die-casting failed prematurely because of a number of parallel cracks on the working surface. These cracks were of a mechanical nature related to incorrect microstructural banding orientation of the die core and related to improper heat treatment. The microstructural banding orientation was determined by metallographic examination of the specimens, which were cut from the dies along the three axes of the coordinate system. Scanning electron microscopy (SEM) examination of the fracture surfaces and along the crack path (including energy dispersive spectroscopy (EDS) analysis) indicated that the root cause of the premature cracking of the dies was improper heat treatment (quenching and tempering conditions). Additionally, resistance to fracture of the investigated specimens, as measured by the Charpy V-notch test, was five times lower than that required for the desired hardness.
Keywords: die failure; die-casting; hot-work tool steel; heat treatment

Dwie identyczne matryce do ciśnieniowego odlewania stopów aluminium zostały przedwczesnie wycofane z eksploatacji z powodu wystąpienia na ich powierzchniach roboczych szeregu równoległych pęknięć. Kierunek propagacji pęknięć pokrywał się z kierunkiem pasmowości mikrostrukturalnej a samo tworzenie się pęknięć było skutkiem niewłaściwej obróbki cieplnej matryc. Stwierdzono nieprawidłową orientację geometryczną matrycy względem kierunku włókien struktury pierwotnej. Badania przy użyciu skaningowego mikroskopu elektronowego z wykorzystaniem techniki EDS wykazały, że przyczyną powstawania pęknięć matryc była nieprawidłowa przeprowadzona obróbki cieplna matryc.

1. Introduction

The service life of die-casting dies might vary from 20 000 to 250 000 parts [1]. Among the many factors affecting their service life, the main ones are: die manufacturing (tolerance, surface finish, stress, manufacturing process), work-piece requirement (tolerance, surface finish), work-piece material (characteristics and temperature), die structure (runner system and overflows, cooling lines, ejector system), die-casting process parameter (temperature, pressure, time, lubrication), die geometry and surface quality (draft angle fillet, corners, deformation, surface quality), die-material (wear resistance, hardness, strength, fracture toughness, thermal conductivity, thermal expansion) and heat treatment [2]. The majority of dies for aluminium die-casting fail because of surface heat checks (parallel cracks forming a pattern on the die surface) caused by thermal fatigue [3–9]. The understanding of the effect of steel chemistry on the precipitation sequence and the stability of the carbides during heat treatment and its effect on the temper resistance led to the development of Dievar hot work steel, primarily to improve the heat checking and gross cracking resistance [10]. The heat treatment of Dievar steel is simplified due to the good hardenability (Fig. 1) but it should not be tempered in the range 500-550°C, in order to avoid temper embrittlement (Fig. 2).

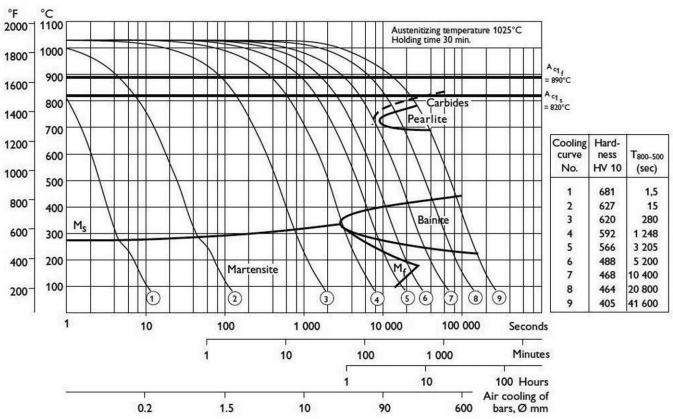

Fig. 1. Continuous cooling transformation diagram of hot work Dievar steel [11]

This paper investigates two damaged dies (surface parallel cracks, indicated by arrows in Fig. 3) that failed after a few thousand shots, instead of after the guaranteed one hundred thousand shots.

* AGH UNIVERSITY OF SCIENCE AND TECHNOLOGY, FACULTY OF METAL ENGINEERING, AND INDUSTRIAL COMPUTER SCIENCE, AL. A. MICKIEWICZA 30, 30-059 KRAKÓW, POLAND

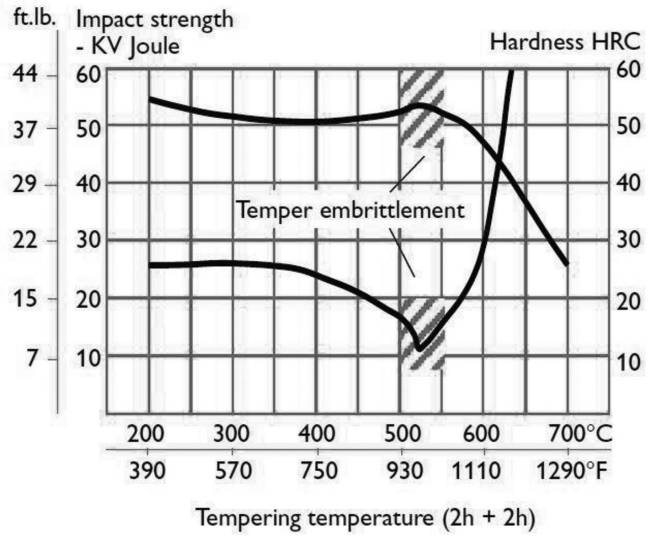

Fig. 2. Effect of tempering temperature on room temperature impact energy [11]

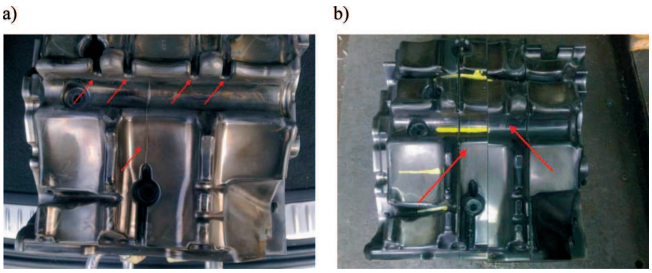

Fig. 3. Surface cracks of dies A (a) and B (b) that failed after a few thousand shots

2. Experimental procedure

Samples from the damaged dies were cut for metallographic, scanning electron microscope (SEM), dilatometric and fracture toughness investigations. For both dies, the samples were geometrically oriented along the three axes of the coordinate system, in which the X-axis was parallel to the direction of the cracks, as shown in Fig. 4.

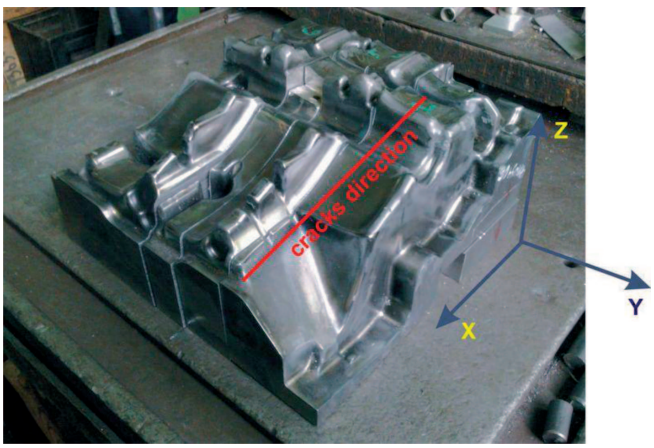

Fig. 4. Coordinate system orientation with respect to direction of surface cracks (red line)

For the metallography, the light microscope Zeiss Axiovert 200MAT was used. The hardness of the specimens was determined by the Rockwell device and the fracture toughness was tested on Charpy V-notched specimens. Fracture surfaces and crack paths were investigated by use of the Hitachi SU-70 SEM equipped with an Energy Dispersive X-ray Spectrometer, which provides chemical analysis of the field of view. A high-resolution RITA L78 dilatometer was used to determine the thermal expansion coefficients along the three axes of the used coordinate system. The chemical composition of the investigated hot work steel was determined by using a Foundry-Master optical emission spectrometer.

3. Results and discussion

The chemical composition of the investigated steel (die A, in wt. %) was 0.32% C, 0.22% Si, 0.44% Mn, 4.71% Cr, 2.17% Mo and 0.58% V and meets the Dievar steel manufacturer requirements [11]. The microstructural banding orientation of the investigated dies can be seen in the macroscopic images of etched metallographic specimens for the XY, XZ and YZ planes (see Fig. 4), which are presented in Fig. 5. The appearance of the microstructural banding (fibrous microstructure of steel) is caused by the segregation of substitutional alloying elements during the dendritic solidification and is affected by subsequent plastic deformation. As shown in Fig. 5, for both dies, the microstructural banding direction is parallel to the X-axis of the coordinate system used, which is also the direction of surface crack propagation. A banding structure of the dies was also observed at higher magnification during the microscopic examination. The results of these observations are shown in Fig. 6. As all observed surface cracks (for both dies) were parallel to the X-axis, it is clear that such a geometrical orientation of the dies with respect to the microstructural banding promotes crack propagation. However, such microstructural banding, as presented in Fig. 5 and Fig. 6, is acceptable according to the North American Die Casting Association industry standard [12] but the banding direction does not meet the requirements of the manufacturer's design assumptions.

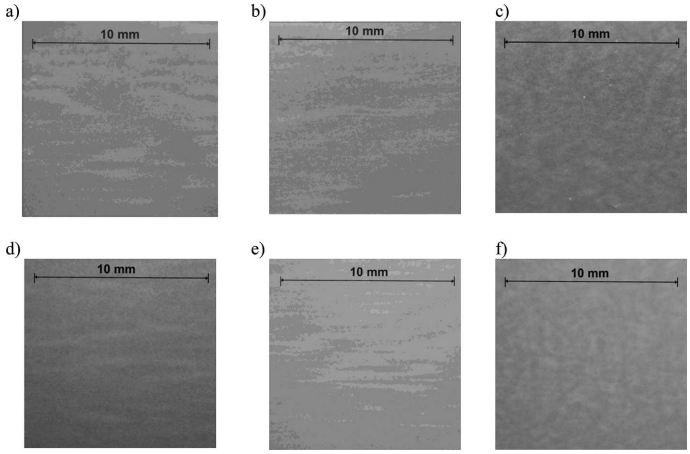

Fig. 5. Macroscopic images of etched metallographic specimens, etched with 2% nital, a) die A XY plane, b) die A XZ plane, c) die A YZ plane, d) die B XY plane, e) die B XZ plane, f) die B YZ plane

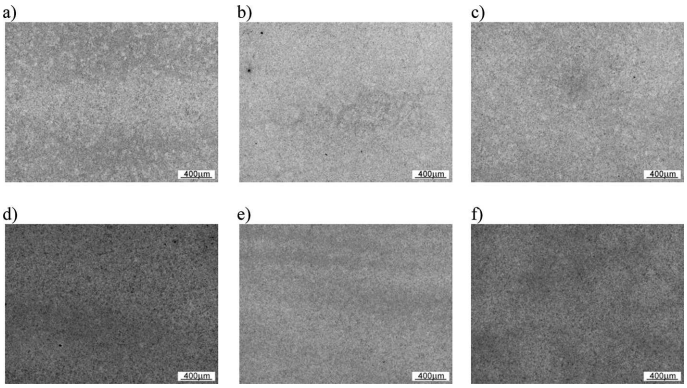

Fig. 6. Microscopic evidence of microstructural banding, etched with 2% nital, a) die A XY plane, b) die A XZ plane, c) die A YZ plane, d) die B XY plane, e) die B XZ plane, f) die B YZ plane

The question remains whether such an orientation could be responsible for crack nucleation on the surfaces of the dies. In the case of die A, selected for further study, it was found that nucleation of one of the cracks took place at the cooling hole edge, as shown in Fig. 7.

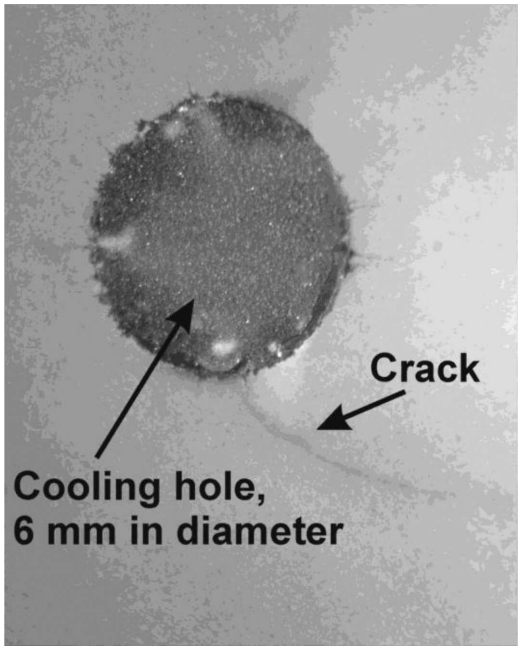

Fig. 7. Crack origin at the edge of cooling hole

Macroscopic observation of the cooling hole cross section (Fig. 7) revealed that around the edge of the hole, many fine cracks had started. Microscopic images of some of these are presented in Fig. 8.

The die microstructure is typical for Dievar steel after quenching and tempering. Light microscopy studies did not confirm the presence of surface decarburisation or wear traces. It was confirmed that the surface and bulk microstructures are similar. SEM studies revealed carbides precipitated along the prior austenite grain boundaries, as shown in Fig. 9. The use of the higher accelerating voltage allowed observation of another type of carbides, precipitated inside the prior austenite grains – transgranular carbides (Fig. 10).

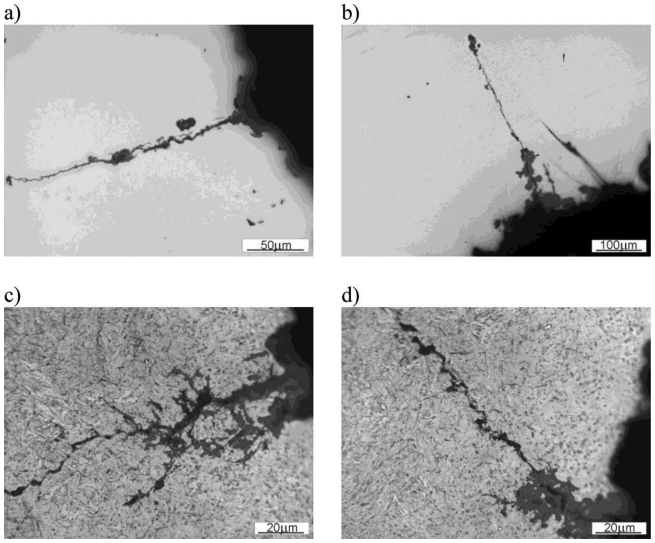

Fig. 8. Microscopic images of cracks nucleated at the edge of cooling hole: a), b) – not etched, c), d) – etched with 2% nital

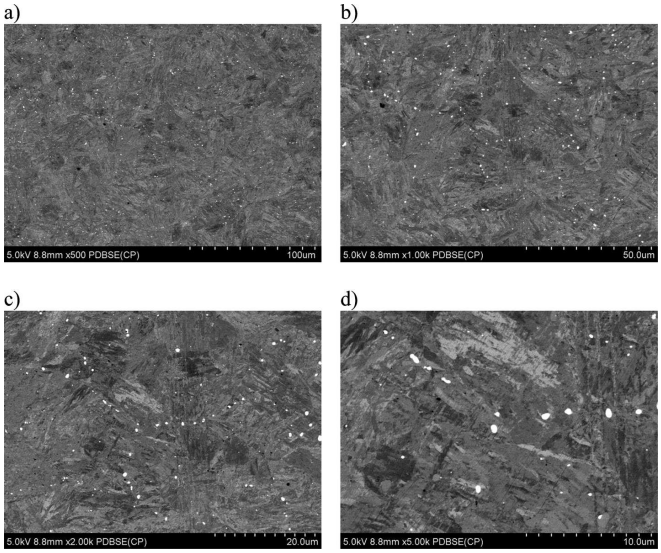

Fig. 9. SEM images of tempered martensite microstructure of investigated steel, accelerating voltage 5 kV

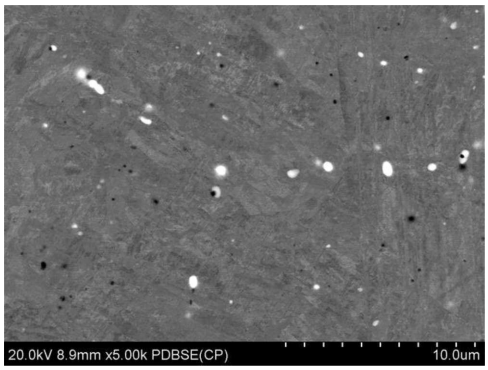

Fig. 10. SEM image of investigated microstructure presented in Fig. 9d with higher accelerating voltage 20 kV

SEM energy dispersive spectroscopy (EDS mapping) of the carbide-forming elements: chromium, molybdenum and vanadium, performed for an area shown in Fig. 10 (not etched

specimen), allowed the presence of vanadium carbides (MC, dark phase in Fig. 11a) and molybdenum carbides (M_2C – light phase in Fig. 11a) to be determined. The presence of the chromium rich regions shown in Fig. 11d, forced the authors to perform similar studies for the etched specimen (Fig. 12); however, in Fig 11a, a non-etched specimen, the chromium carbides were not seen. In Fig. 12a, it can be observed that there is a large amount of coarsened chromium carbides (Fig. 12d), probably of type $M_{23}C_6$ and/or M_7C_3.

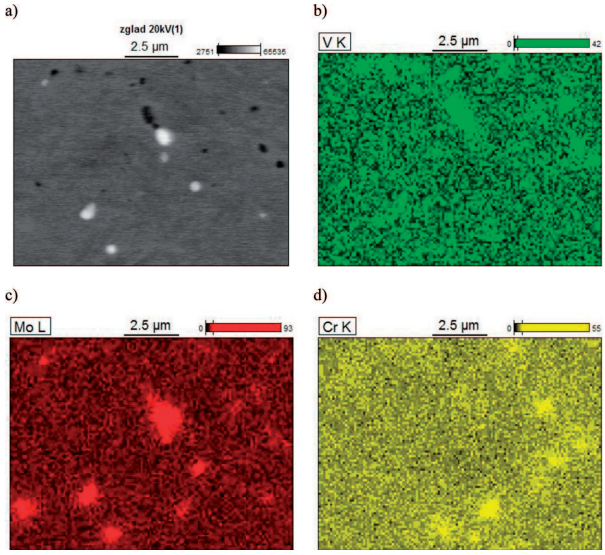

Fig. 11. Energy dispersive element mapping performed of area shown in Fig. 10, a) microstructure, b) vanadium mapping, c) molybdenum mapping, d) chromium mapping

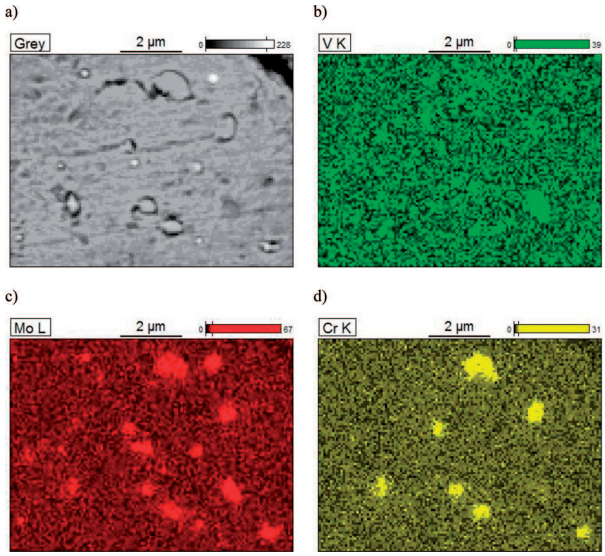

Fig. 12. Energy dispersive element mapping performed for etched specimen, a) microstructure, b) vanadium mapping, c) molybdenum mapping, d) chromium mapping

According to [13], the presence of chromium $M_{23}C_6$ and M_7C_3 carbides in Dievar steel microstructure is because of the high austenitising temperature. As stated in [13], a tempering resistance test of Dievar steel at four different heat treatments: 1020, 1060, 1100 and 1150°C, showed that an increased austenitising temperature improves the temper resistance (after hardening, all investigated materials were tempered to an equal hardness 470±10 HV30).

The results of microscopic examinations show that cracks presented in Fig. 7 propagate along prior austenite grain boundaries and/or tempered martensite lath boundaries, as shown in Fig. 13.

SEM observations were also made for the fracture surface at the origin of the crack presented in Fig. 7. The results of this investigation are shown in Fig. 14 and Fig. 15. As can be observed, the crack initiation occurred at the edge of the cooling hole and further crack propagation took place in stages, probably corresponding to the die-casting cycles (the so-called "shots"). Fig. 16 shows a transgranular fracture mode of the above-mentioned stages, separated by a dimple fracture area (Fig. 16a) with friction traces (Fig. 16b).

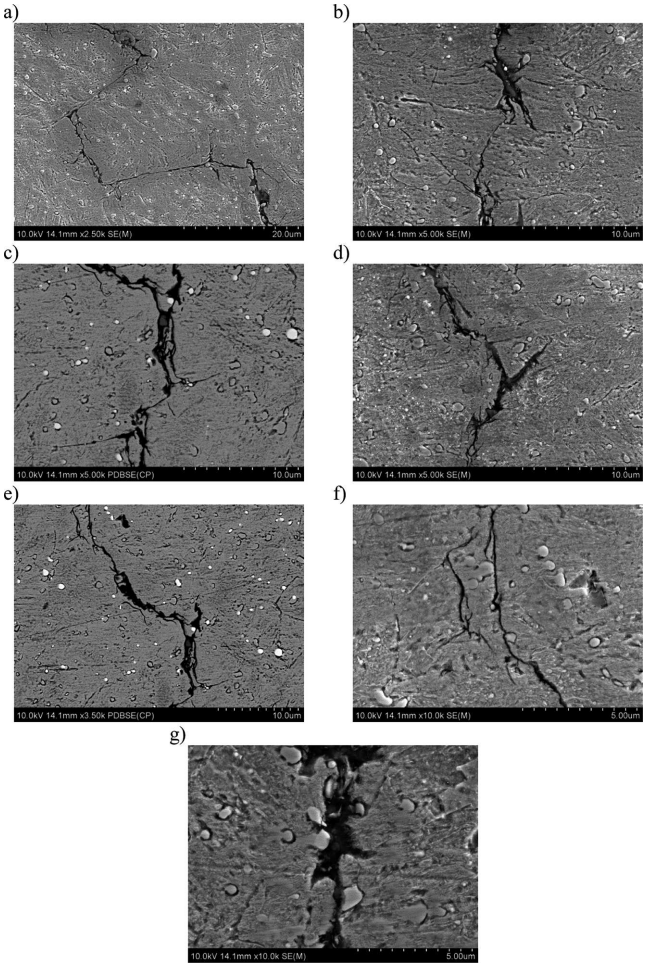

Fig. 13. SEM images of propagation path of crack presented in Fig. 7, a-g) different crack areas

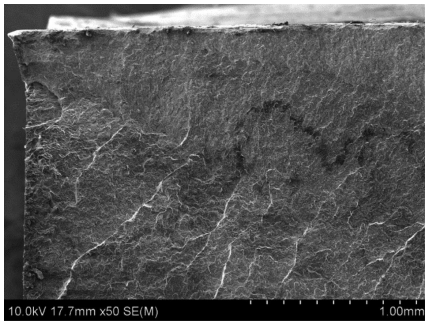

Fig. 14. SEM image of fracture surface of crack presented in Fig. 7, close to the cooling hole (crack origin)

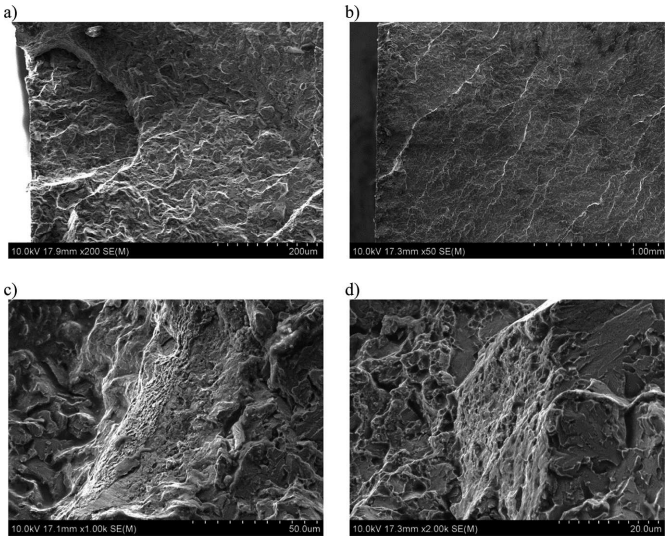

Fig. 15. SEM images of transgranular fracture mode separated by dimple fracture area, a) general view, b) crack origin, c-d) transition region

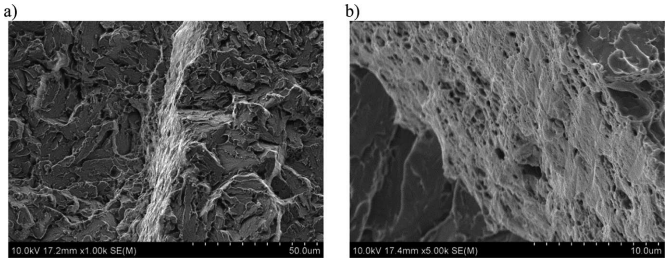

Fig. 16. SEM images of fracture surface a) brittle crack propagation stages, b) dimple fracture transition area

The results of SEM studies (brittle fracture mode) suggest that the fracture toughness of the investigated dies might be not as high as guaranteed by the producer (impact energy approximately 27 J at room temperature for the required Rockwell hardness 47 HRC) after quenching and tempering [11].

In this study, the Rockwell hardness tests were performed to measure the hardness of the failed dies. The mean hardness value of the investigated dies was equal to 47 HRC (standard deviation 0.44); thus, the hardness level meets the requirements for the hardness range of dies for aluminium alloy die-casting [11]. The hardness test is commonly used to verify heat treatment; however, in the case of Dievar steel, the verification of heat treatment should be conducted by a combination of hardness and fracture toughness. Such a statement is supported by the effect of tempering temperature on the room temperature impact energy of Dievar steel [11]. In Fig. 2, it can be observed that tempering in the range of 500-550°C for the required final hardness will result in a lower toughness.

Therefore, in this study, the fracture toughness was determined on Charpy V-notched specimens with both planes oriented parallel to the XY, XZ and YZ planes of the used coordinate system (Fig. 4). The results of the Charpy impact energy test show that the fracture toughness of the investigated dies is five times lower than that required for the desired hardness (27 J for 47 HRC [11]): XY plane 4.8 J, XZ plane 5.4 J and YZ plane 5.3 J (mean values).

Thus, it can be concluded that the very low fracture toughness of the investigated dies was the main cause of the observed cracks.

4. Conclusions

The present study has demonstrated that:

- The crack initiation occurred at the edge of the cooling hole and further crack propagation took place in stages, probably corresponding to the die-casting cycles.
- All observed surface cracks (for both dies) were parallel to the revealed microstructural bands, which promote crack propagation.
- Hardness of the investigated dies met the requirements for the hardness range of dies for aluminium alloy die-casting.
- The results of the Charpy impact energy test show that the fracture toughness of the investigated dies is five times lower than that required for the desired hardness.
- The root cause of premature cracking of dies was improper heat treatment (temper embrittlement).

REFERENCES

[1] J.R. Davis, (ed.), Tool Materials. ASM Specialty Handbook, ASM International, 1995.
[2] Z.-X. Jia, J.-Q. Li, Y.Q. Wang, Cover die service life improvement by biomimetic laser-remelting process and CAE simulation. International Journal of Advanced Manufacturing Technology, 1-9 (2012).
[3] Y. Wang, A study of PVD coatings and die materials for extended die-casting die life. Surfaces and Coatings Technology **94-96**, 60-63 (1997).
[4] A. Srivastava, V. Joshi, R. Shivpuri, Computer modelling and prediction of thermal fatigue cracking in die-casting tooling. Wear **256**, 38-43 (2004).
[5] B. Kosec, M. Sokovic, G. Kosec, Failure analysis of dies for aluminium alloys die-casting. Achievements in Mechanical and Materials Engineering, 339-342 (2005).
[6] B. Kosec, Failures of dies for die-casting of aluminium alloys. Metalurgija **47**(1), 51-55 (2008).
[7] M. Muhic, J. Tusek, F. Kosel, D. Klobcar, Analysis of die casting tool material. Journal of Mechanical Engineering **56**(6), 351-356 (2010).
[8] M. Muhic, J. Tusek, F. Kosel, D. Klobcar, M. Pleterski, Thermal fatigue cracking of die-casting dies. Metalurgija **49**(1), 9-12 (2010).
[9] D. Klobcar, L. Kosec, B. Kosec, J. Tusek, Thermo fatigue cracking of die casting dies. Engineering Failure Analysis **20**, 43-53 (2012).
[10] K.K. Iyer, Dievar – for improved die performance of large tools. Metalworld **5**, 23-25 (2008).
[11] Uddeholm Dievar. Uddeholms AB Sweden brochure, Edition 9, 2012.
[12] NADCA Die Material Committee: Special Quality Die Steel & Heat Treatment Acceptance Criteria for Die Casting Dies, NADCA #207-2008, North America Die Casting Association, 2008.
[13] J. Sjöström, Chromium martensitic hot-work tool steels – damage, performance and microstructure, Doctoral thesis, Karlstad University, Sweden, 2004.

Received: 20 September 2012.